6378 *J. Med. Chem.* **2010,** *53,* 6378–6385
DOI: 10.1021/jm100545a

Journal of Medicinal Chemistry
Article

Synthesis and Characterization of Nitroimidazole Derivatives for ^{68}Ga-Labeling and Testing in Tumor Xenografted Mice

Lathika Hoigebazar,[†,‡] Jae Min Jeong,*[,†,‡] Soo Young Choi,[§] Jae Yeon Choi,[†,‡] Dinesh Shetty,[†,‡] Yun-Sang Lee,[†,‡] Dong Soo Lee,[†,‡] June-Key Chung,[†,‡] Myung Chul Lee,[†,‡] and Young Keun Chung[§]

[†]*Department of Nuclear Medicine, Radiation Applied Life Sciences, Institute of Radiation Medicine, Seoul National University College of Medicine, 101 Daehangno, Jongno-gu, Seoul 110-744, Korea,*
[‡]*Cancer Research Institute, Seoul National University College of Medicine, Seoul 110-744, Korea, and*
[§]*Intelligent Textile System Research Centre and Department of Chemistry, Seoul National University, Seoul, Korea*

Received May 5, 2010

Radiolabeled nitroimidazole (NI) derivatives have been used for imaging hypoxic tissues. We synthesized NI derivatives conjugated with bifunctional chelating agents such as 1,4,7-triazacyclononane-1,4,7-triacetic acid (NOTA) and isothiocyanatobenzyl-NOTA (SCN-NOTA) via ethyleneamine bridge by formation of amide and thiourea bond, respectively. We proved that amide oxygen of Ga-NOTA-NI contributes to the formation of metal complex by X-ray crystallography. We labeled them with ^{68}Ga and found that both ^{68}Ga-NOTA-NI and ^{68}Ga- SCN-NOTA-NI were labeled in high efficiency (>96%) and were stable at room temperature in the prepared medium and at 37 °C in human serum. In vitro cell uptake experiments using CHO and CT-26 cell lines showed significantly increased uptakes of both of the agents in hypoxic condition. Biodistribution study in CT-26 xenografted mice showed increasing tumor to muscle ratios. ^{68}Ga-NOTA-NI showed lower intestine uptake than ^{68}Ga-NOTA-SCN-NI due to hydrophilicity. Also, ^{68}Ga-NOTA-NI showed higher tumor uptake than ^{68}Ga-NOTA-SCN-NI in an animal PET study. In conclusion, we successfully developed ^{68}Ga labeled NI derivatives for hypoxic tissue imaging.

Introduction

The detection of hypoxia is important for treatment planning, such as in cases of cancer or myocardial ischemia.[1−3] Since NI[a] drugs have wide clinical applications, especially for the targeting of hypoxic tumors,[4−16] the inclusion of the NI moiety has become an important consideration during drug development. In particular, 2-NI (**1**) can be reduced to form a reactive chemical species, which can bind to cell components in the absence of sufficient oxygen,[5,17−19] and thus, the development of radiolabeled NI derivatives for the imaging of hypoxia remains an active field of research to improve cancer therapy result.

The positron emission tomography (PET) tracer [^{18}F]fluoromisonidazole (FMISO)[20−23] (Figure 1) was the first NI agent used for imaging hypoxia. However, it requires at least a 2 h wait before image acquisition due to its slow washout from normoxic tissues, which is a serious fault because ^{18}F labeled agents have relatively short half-lives (110 min).[18] Agents more hydrophilic than [^{18}F]FMISO have been developed, such as [^{18}F]fluoroerythronitroimidazole (FETNIM),[24,25] [^{18}F]1-α-D-(2-deoxy-2-fluoroarabinofuranosyl)-2-nitroimidazole (FAZA),[6,8,18,26−28] [^{18}F]2-(2-nitro-1*H*-imidazol-1-yl)-*N*-(2,2,3,3,3-pentafluoropropyl)acetamide (EF-5),[16,29−32] and [^{124}I]1-α-D-(2-deoxy-2-fluoroarabinofuranosyl)-2-nitroimidazole (IAZA),[7] to improve target to nontarget ratio by increasing excretion rates (Figure 1).

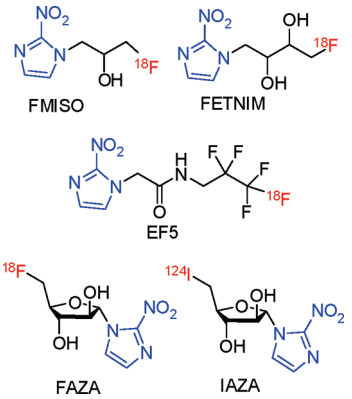

Figure 1. NI agents previously developed for the imaging of hypoxia.

Furthermore, although a ^{64}Cu-diacetyl-bis(N_4-methylthiosemicarbazone) (ATSM) has been developed that is cleared rapidly from normoxic tissues, the production of ^{64}Cu requires

*To whom correspondences should be addressed. Phone: 82-2-2072-3805. Fax: 82- 2-745-7690. E-mail: jmjng@snu.ac.kr.

[a] Abbreviations: NI, nitroimidazole; SCN-NOTA, isothiocyanatobenzyl-1,4,7-triazacyclononane-1,4,7-triacetic acid; PET, positron emission tomography; FMISO, fluoromisonidazole; FETNIM, fluoroerythronitroimidazole; FAZA, 1-α-D-(2-deoxy-2-fluoroarabinofuranosyl)-2-nitroimidazole; EF-5, 2-(2-nitro-1*H*-imidazol-1-yl)-*N*-(2,2,3,3,3-pentafluoropropyl)acetamide; IAZA, 1-α-D-(2-deoxy-2-fluoroarabinofuranosyl)-2-nitroimidazole; ATSM, diacetyl-bis(N_4-methylthiosemicarbazone); DMF, dimethylformamide; TLC, thin layer chromatography; DCC, *N*,*N*′-dicyclohexylcarbodiimide; ITLC-SG, instant thin layer chromatography silica gel; TEA, triethylamine; RP-HPLC, reverse phase-high performance liquid chromatography.

 Published on Web 08/06/2010

Scheme 1. Synthesis of NOTA-2-NI-*N*-ethylamine (**3**) and SCN-NOTA-2-NI-*N*-ethylamine (**4**)[a]

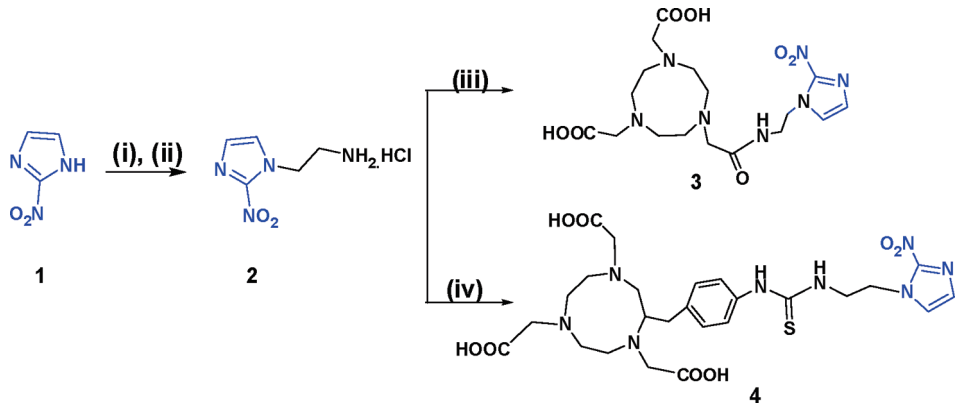

[a] (i) *tert*-Butyl 2-bromoethylcarbamate, K_2CO_3, DMF, room temp; (ii) HCl/MeOH, room temp; (iii) NOTA, H_2O/DMF, DCC, pyridine, room temp, overnight; (iv) SCN-NOTA, $CHCl_3$, TEA, room temp, overnight.

a special solid target and expensive target material, and hence, its use is likely to be limited.[33−35]

In fact, the productions of ^{18}F, ^{64}Cu, and ^{124}I require cyclotron and chemical processing, which are expensive and difficult to operate and maintain. In the present study, we undertook to develop ^{68}Ga-labeled NI derivatives for hypoxia imaging by PET because ^{68}Ga can be produced using a relatively easily available generator system,[36−39] and a simple kit can be produced to help routine labeling procedure.[40]

Unlike the radioactive halogens, the labeling of ^{68}Ga requires the use of bifunctional chelating agents that can conjugate to biomolecules and form thermodynamically stable complexes with Ga. The triazamacrocyclic ligand, NOTA, has been reported to form highly stable complexes with small cations like Ga^{3+},[41,42] and thus, various peptides conjugated with NOTA derivatives have been developed.[43,44] In previous studies, ^{67}Ga-labeled NI derivatives of NOTA were prepared with a functional group at the ring ethylene backbone.[45] In the present study, we synthesized a new NOTA-NI (**3**) conjugate for labeling with ^{68}Ga. In addition, we also synthesized SCN-NOTA-NI (**4**) conjugate as a control and compared the in vivo and in vitro properties of these two derivatives.

In the Ga-NOTA complex, all three carboxyl groups of NOTA bind with gallium. However, in **3**, one of these carboxyl groups formed an amide group, and thus, only two carboxyl groups remain for gallium chelation. Accordingly, we wondered whether **3** forms a stable complex with gallium, and if so, which atom of the amide bond would bind with gallium. To confirm this, we performed X-ray crystallography using Ga-**3** crystals produced at pH 3 and pH 5 in aqueous solution.

Results and Discussion

Chemistry. To synthesize the ^{68}Ga-labeled nitroimidazole derivatives **3** and **4**, we prepared 2-(2-nitroimidazolyl)ethylamine (**2**) in the form of an HCl salt (Scheme 1). *tert*-Butyl 2-(2-nitroimidazolyl)ethylcarbamate was synthesized by the N-alkylation of **1** with *tert*-butyl 2-bromoethylcarbamate in MeCN (35%). K_2CO_3 was used as the base, and the reaction was performed at room temperature overnight. We observed that conjugation yields increased up to 80% when this reaction was carried out in dimethylformamide (DMF), which we attribute to be the higher solubility of **1** in DMF. The crude product was purified by recrystallization from EtOAc.

Table 1. Crystallographic Experimental Data of Ga-**3**

parameter	
empirical formula	$C_{18}H_{24}GaN_7O_{10}$
formula weight	568.16
temperature	293(2) K
wavelength	0.710 73 Å
crystal system	orthorhombic
space group	*Pbca*
unit cell dimensions	a = 14.1280(5) Å, α = 90°
	b = 14.8639(5) Å, β = 90°
	c = 21.2809(7) Å, γ = 90°
volume	4468.9(3) Å^3
Z	8
calculated density	1.689 Mg/m^3
absorption coefficient	1.304 mm^{-1}
F(000)	2336
crystal size	0.51 mm × 0.38 mm × 0.11 mm
range for data collection	2.40−27.51°
limiting indices	$-18 \le h \le 18$, $-19 \le k \le 19$, $-27 \le l \le 27$
reflections collected/unique	8963/5048 [R(int) = 0.0345]
completeness to θ = 27.51	98.2%
absorption correction	empirical
max and min transmission	0.8698 and 0.5560
refinement method	full-matrix least-squares on F^2
data/restraints/parameters	5048/0/326
goodness-of-fit on F^2	1.059
final R indices [$I > 2\sigma(I)$]	R1 = 0.0398, wR2 = 0.0966
R indices (all data)	R1 = 0.0686, wR2 = 0.1076
extinction coefficient	0.0038(4)

The subsequent deprotection of the amine was achieved using 1.25 M HCl in methanol (MeOH), which gave **2** in high yield (84%). Reaction completion was confirmed by thin layer chromatography (TLC), and the crude product was purified by recrystallization from MeOH.

To synthesize **3**, acid/amine coupling was carried out in a water and DMF mixture (1:1 vol/vol) using *N*,*N*′-dicyclohexylcarbodiimide (DCC) as a coupling agent in the presence of pyridine. To synthesize **4**, SCN-NOTA and amine were conjugated in chloroform ($CHCl_3$) using triethylamine (TEA) as a base. The formation of products during both reactions was monitored by mass spectrometry in electrospray ionization positive mode (MS/ESI$^+$). Products were purified by reverse phase high performance liquid chromatography (RP-HPLC) to obtain products **3** and **4** at yields of 52% and 73%, respectively. According to mass analysis, we did not find even a trace amount of disubstituted or

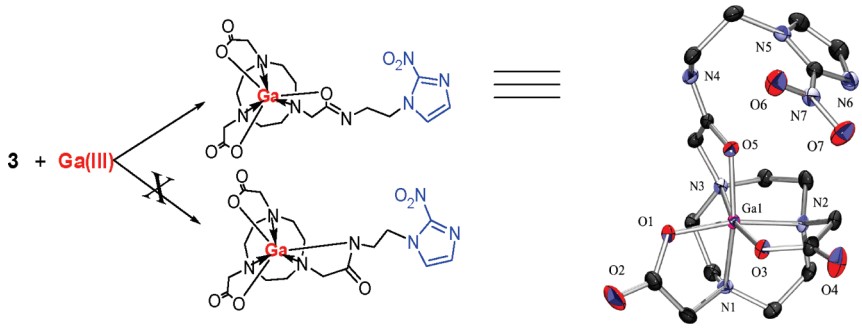

Figure 2. ORTEP drawing of Ga-**3**. Hydrogen atoms and counterions have been omitted for clarity. Gallium binds with oxygen atom of amide bond and not with nitrogen.

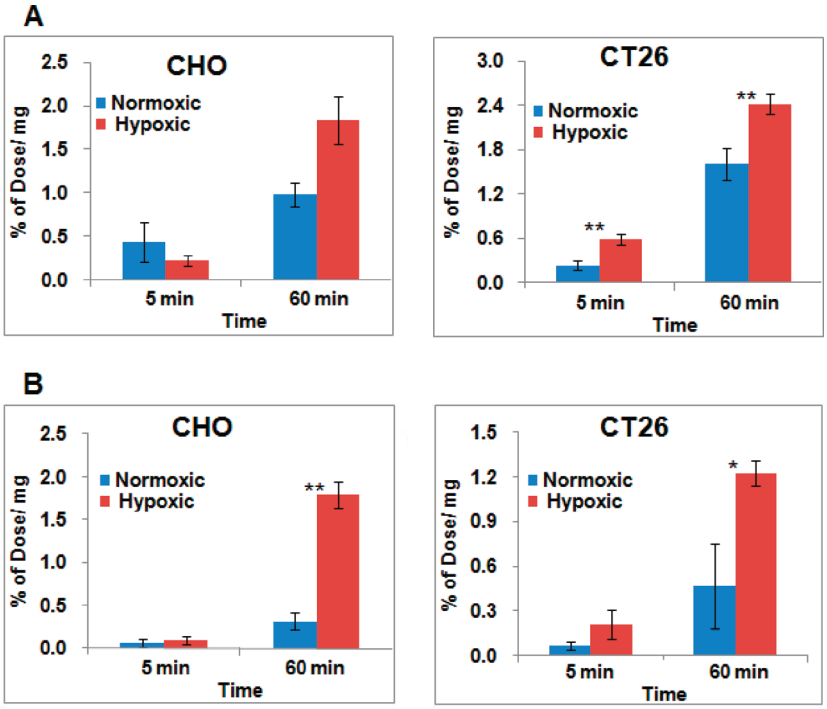

Figure 3. In vitro cell uptake studies of (A) ^{68}Ga-**3** and (B) ^{68}Ga-**4** under normoxic and hypoxic conditions by CHO and CT26 cells. p values represent comparisons between uptakes under normoxic and hypoxic conditions (t-test): (**) $p < 0.01$, (*) $p < 0.05$, $n = 4$ at each time point.

trisubstitued product of NOTA-NI, as was expected by the reaction of acid amine coupling (Supporting Information p S9).

Crystallography. Crystallography was performed only on Ga-**3** and not on Ga-**4** because **4** possesses three carboxyl groups and thus is deemed to be almost certain to form an octahedral crystal structure with gallium. However, as mentioned above, **3** has only two carboxyl groups (one formed an amide bonded to ethylnitroimidazole), and thus, it was not clear whether it would form a stable complex with gallium.

Complexation of Ga(III) with **3** was performed in aqueous solution by mixing stoichiometric amounts of **3** and $Ga(NO_3)_3 \cdot xH_2O$ at pH 3 or 5. Complex formation was monitored by MS/ESI$^+$, and the Ga-**3** produced was purified by RP-HPLC. Crystals of Ga-**3** were obtained by allowing the water solution to evaporate slowly at room temperature and analyzed using graphite-monochromated Mo Kα radiation and an Enraf-Nonius CCD single-crystal X-ray diffractometer at room temperature (data are summarized in Table 1). We investigated the crystal structure to ensure the possibility of metal coordination with either amide nitrogen (N4) or oxygen (O5). Both crystals at pH 3 and 5 produced identical diffraction patterns, and gallium was found to be coordinated with the amide oxygen (O5) of NOTA (Figure 2). Direct binding of NI residue and gallium atom was not observed. This is important because the intact NI group is essential for the in vivo binding of the agent in hypoxic tissue. In addition, we found one counterion (CO_3^{2-}) per unit cell derived from Na_2CO_3 buffer used during complexation. Ga-**3** complex showed *Pbca* symmetry with eight molecules per unit cell (Z). Three nitrogen atoms (from the backbone ring) and three oxygen atoms (two from the carboxylic acid and one from the amide oxygen of the modified carboxylic acid) were found to coordinate with the gallium atom to produce a distorted octahedral geometry, which was evidenced by a compression of N−Ga−N angles (average 84.7°) and expansion of O−Ga−O angles (average 93.3°). The average bond angle of trans N−Ga−O was 166.5°, which is similar to that found in Ga-NOTA (167°).[41,46,47] The average Ga−N bond length in Ga-**3** was 2.09 Å, which is the same as that of Ga-NOTA, and the average Ga−O bond length was 1.94 Å (1.93 Å for Ga-NOTA).[47]

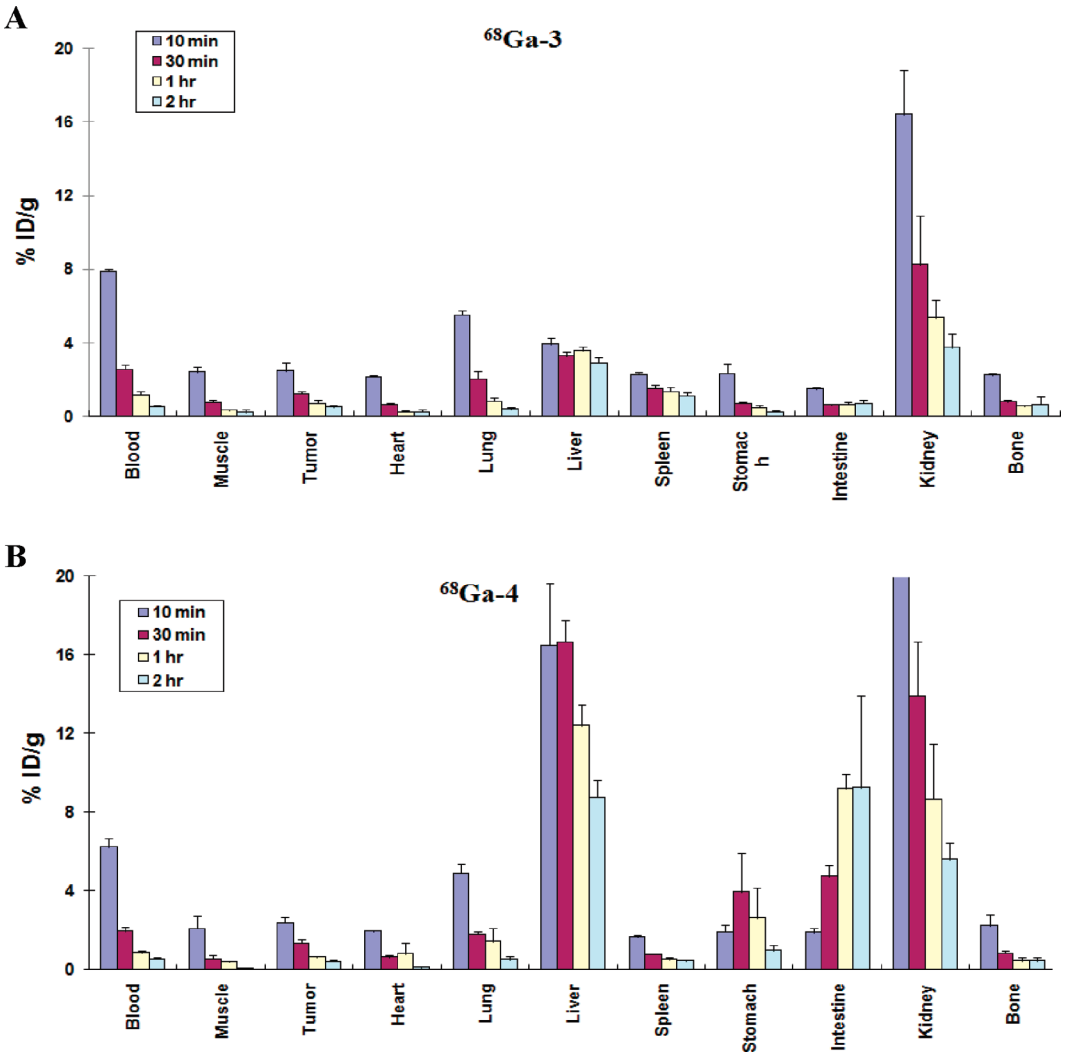

Figure 4. Histograms showing biodistribution at 10, 30, 60, and 120 min postinjection of (A) ^{68}Ga-**3** and (B) ^{68}Ga-**4** in mice bearing CT-26 xenograft which are reported as mean percentage injected dose per gram tissue ± standard deviation (% ID/g ± SD); $n = 4$ at each time point.

Radiochemistry. ^{68}Ga was eluted from a ^{68}Ge/^{68}Ga-generator using 0.1 N HCl. Radiolabeling was conducted at pH 3 in a boiling water bath for 10 min. Free $^{68}Ga^{3+}$ was removed using an alumina cartridge. Labeling efficiencies were checked by instant thin layer chromatography silica gel (ITLC-SG) (Supporting Information Figure 1) and found to be 96.0 ± 0.7% and 96.3 ± 5.5% for ^{68}Ga-**3** and ^{68}Ga-**4**, respectively. Low partition coefficients (log *P*) were observed for ^{68}Ga-**3** (−2.71) and ^{68}Ga-**4** (−2.27), indicating that both of them are hydrophilic. However, ^{68}Ga-**3** was found to be a little more hydrophilic than ^{68}Ga-**4**, which was expected because of the absence of the aromatic ring. Both agents showed low protein binding (0.06 ± 0.02% at 10 min and 0.12 ± 0.04% at 60 min for ^{68}Ga-**3**, 1.66 ± 0.04% at 10 min and 2.45 ± 0.06% at 60 min for ^{68}Ga-**4**), which is desirable for imaging agents, and this finding was also consistent with the literature which reported that ^{68}Ga-labeled NOTA derivatives showed low protein binding.[48] Furthermore, both labeled agents were found to be stable up to 240 min at room temperature (Supporting Information Figure 2).

Cell Uptake Study. CHO (a Chinese hamster ovarian cancer cell line) and CT-26 (a mouse colon cancer cell line) were used for the cell uptake study. Both cell lines showed significantly higher uptakes of ^{68}Ga-**3** and ^{68}Ga-**4** under hypoxic than under normoxic conditions after 1 h (Figure 3). The difference between the uptakes in hypoxic and normoxic conditions was significant in CHO and CT26 cell lines at 60 min (1.8 ± 0.1 times in CHO, 1.5 ± 0.6 times in CT26 for ^{68}Ga-**3**; 5.6 ± 1.5 times in CHO, 2.6 ± 0.3 times in CT26 for ^{68}Ga-**4**). Cell uptake results obtained for ^{68}Ga-**3** and ^{68}Ga-**4** were comparable to those of [^{18}F]FAZA and [^{18}F]FMISO. According to the literature, uptake of [^{18}F]FAZA and [^{18}F]FMISO under hypoxic conditions was increased significantly in comparison to normoxic conditions (1.4 ± 0.3 times for [^{18}F]FAZA and 1.5 ± 0.4 times for [^{18}F]FMISO) at 20 min and (2.7 ± 0.4 times for [^{18}F]FAZA and 3.0 ± 0.6 times for [^{18}F]FMISO) at 100 min.[18]

Animal Studies in Mice Bearing CT-26 Xenografts. For ^{68}Ga-**3** and ^{68}Ga-**4**, biodistribution studies were performed at different time points (10, 30, 60, and 120 min) after intravenous injection of these labeled derivatives (37 KBq) into mice bearing CT-26 xenografts (Figure 4). As the tumors grow, hypoxia essentially builds up.[12,13] So the tumor uptake can be used as an indicator of the agents taken up to hypoxia. The highest uptakes were demonstrated in kidneys (16.43 ± 2.41% ID/g for ^{68}Ga-**3** and 28.53 ± 16.59% ID/g for ^{68}Ga-**4** at 10 min) for both derivatives, indicating that they are probably excreted via kidneys. The higher liver and intestine

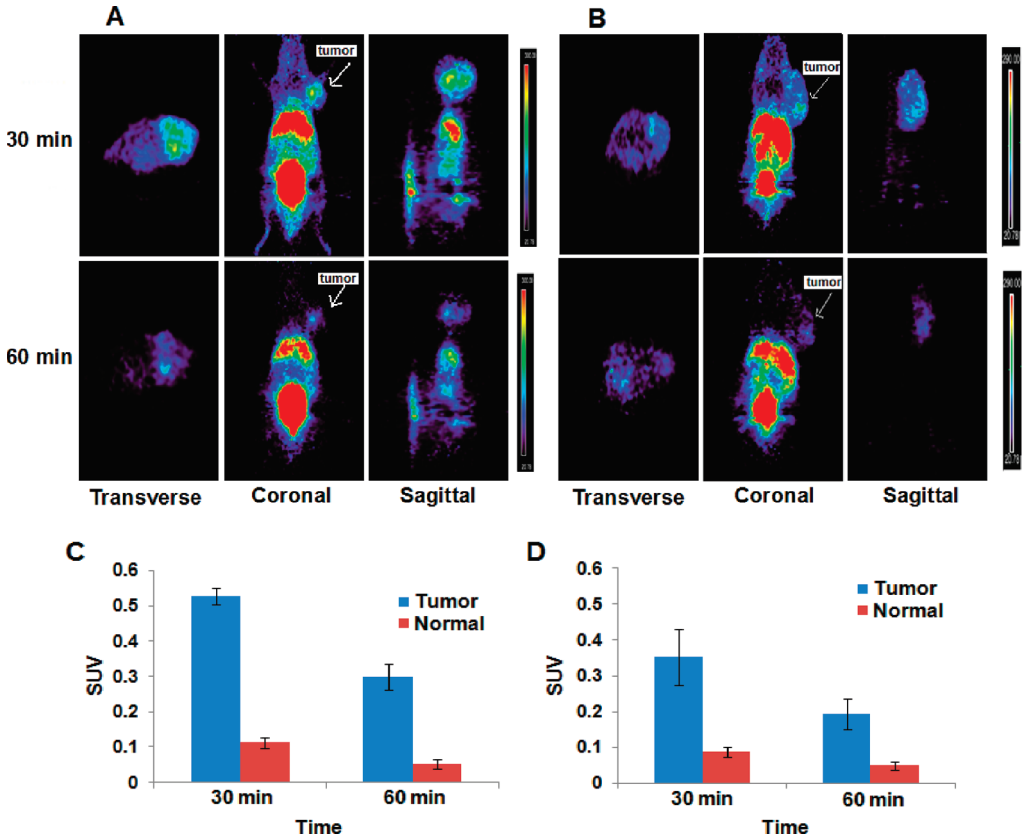

Figure 5. Small animal PET images of mice bearing a CT-26 xenograft on the right shoulder. (A) ^{68}Ga-**3** (13.3 MBq/0.1 mL) and (B) ^{68}Ga-**4** (12.6 MBq/0.1 mL) are injected through tail vein at 30 and 60 min postadministration. (C) and (D) show SUVs for ^{68}Ga-**3** and ^{68}Ga-**4**, respectively. "Normal" indicates muscle.

uptake of ^{68}Ga-4 (12.41 ± 1.09 and 9.21 ± 0.72% ID/g at 1 h, respectively) than ^{68}Ga-3 (3.59 ± 0.21 and 0.66 ± 0.12% ID/g at 1 h, respectively) was attributed to the higher lipophilicity of **4**. The initial tumor uptakes were 2.47 ± 0.47 and 2.37 ± 0.29% ID/g at 10 min postinjection for ^{68}Ga-**3** and ^{68}Ga-**4**, respectively. These activities declined over time for both derivatives. It was 1.25 ± 0.11% ID/g for ^{68}Ga-**3** and 1.34 ± 0.17% ID/g for ^{68}Ga-**4** at 30 min, 0.73 ± 0.18% ID/g for ^{68}Ga-**3** and 0.61 ± 0.06% ID/g for ^{68}Ga-**4** at 60 min, and 0.51 ± 0.10% ID/g for ^{68}Ga-**3** and 0.42 ± 0.07% ID/g for ^{68}Ga-**4** at 120 min. In addition, the tumor to blood uptake ratios of ^{68}Ga-**3** (0.62 ± 0.01) and ^{68}Ga-**4** (0.73 ± 0.12) were less compared to those of [^{18}F]FAZA (3.27)[6] and [^{18}F]FMISO (1.19)[49] at 60 min, whereas the tumor to muscle uptake ratios of ^{68}Ga-**3** (2.13 ± 0.58) and ^{68}Ga-**4** (1.64 ± 0.39) were comparable to those of F-18 labaled NI derivatives (1.69 for [^{18}F]FAZA and 1.65 for [^{18}F]FMISO)[6,49] at the same time point (Figure 4). These results could open the possibility of ^{68}Ga-labeled NI derivatives, especially ^{68}Ga-**3**, for PET hypoxia tumor imaging.

A small animal PET study was performed, and images were obtained at 30 and 60 min after injecting ^{68}Ga-**3** (13.3 MBq/0.1 mL) or ^{68}Ga-**4** (12.6 MBq/0.1 mL) into a mouse bearing CT-26 xenografts via tail vein. Both agents showed high liver, kidney, and bladder uptakes as predicted from the biodistribution study. ^{68}Ga-**3** demonstrated better tumor uptake than ^{68}Ga-**4** (Figure 5). To perform a quantitative analysis, we calculated standardized uptake value (SUV), which is defined as a ratio of tissue radioactivity concentration (MBq/mL) at time T and injected dose (MBq) at the time of injection divided by body weight (g) in PET image. ^{68}Ga-**3** (0.30 ± 0.2) demonstrated a higher SUV value than ^{68}Ga-**4** (0.19 ± 0.1) at 60 min postinjection. From literature SUV values of [^{18}F]FAZA is 0.68 ± 0.2 and [^{18}F]FMISO is 1.07 ± 0.3.[18] The tumor to muscle SUV ratios of ^{68}Ga-**3** and ^{68}Ga-**4** were 5.7 ± 2.5 and 3.95 ± 1.3 at 60 min postinjection, respectively, which were higher than the values of [^{18}F]FAZA (2.4 ± 0.6) and [^{18}F]FMISO (2.7 ± 0.6).[18]

The high uptake of these ^{68}Ga-labeled derivatives in liver and kidney is the drawback of these derivatives, since many tumors are located in abdominal area. To solve these problems, development of a more hydrophilic agent is required because hydrophilic agents generally demonstrate reduced liver uptake and increased kidney excretion rate. If we add carboxyl or hydroxyl groups at the linker between nitroimidazole and NOTA, more hydrophilic agents might be produced. Especially, introduction of carboxyl group would make the product more negatively charged and hence may facilitate the rapid clearance through the kidneys. Or changing the bifunctional chelating agent would be another possibility for improvement.

Conclusion

We successfully synthesized NI conjugates of NOTA via formation of amide (**3**) or thiourea bond (**4**). Furthermore, amide carbonyl was found to participate in the formation of Ga-**3**. Both **3** and **4** were labeled by ^{68}Ga at high yields in a straightforward manner, and both labeled agents were found to be stable and to have low protein binding. ^{68}Ga-**3** was found to have a lower log P value than Ga-**4**, which is attributed to its higher hydrophilicity. ^{68}Ga-**3** and ^{68}Ga-**4** showed elevated uptakes in hypoxic cells in vitro. In addition,

biodistribution and PET studies showed that both have high tumor to muscle ratios. Thus, both agents, but especially ^{68}Ga-**3**, were found to be potential agents for the PET imaging of hypoxic tissue.

Experimental Section

Chemistry. NOTA was purchased from ChemaTech (Dijon, France) and SCN-NOTA from Futurechem (Seoul, Korea). HPLC grade MeCN and EtOH were purchased from Fischer Scientific Korea Ltd. (Seoul, Korea). All other reagents were purchased from Sigma-Aldrich (St. Louis, MO) and were used without further purification. ^{68}Ge/^{68}Ga generator was purchased from Eckert and Ziegler (Berlin, Germany). ^{1}H NMR and ^{13}C NMR spectra were recorded on a AL 300 FT NMR spectrometer (300 MHz for ^{1}H and 75 MHz for ^{13}C; Jeol Ltd., Tokyo, Japan) and were referenced internally using residual solvent signals. ^{1}H NMR peaks are described as s for singlet, d for doublet, t for triplet, q for quartet, m for multiplet, or br for broad, and coupling constants are presented in Hz. ^{1}H chemical shift values are expressed as δ values (parts per million) relative to tetramethylsilane (the internal standard). HPLC was performed using a XTerra RP18 (10 mm × 250 mm) column (Waters Corporation, Milford, MA). The solvent systems used were A (10 mM HCl in H_2O), B (H_2O), C (MeCN), and D (EtOH), and the flow rates for analytical and preparative HPLC were 1 and 5 mL/min with suggested linear gradients, respectively. The purities of synthesized compounds were confirmed to be higher than 95% by analytical HPLC (Supporting Information). ESI data were recorded on a Waters ESI ion trap spectrometer (Milford, MA) in positive ion detection mode and high resolution mass spectra (HRMS) on a Jeol, JMS-AX505WA, HP5890 series II spectrometer by fast atomic bombardment (FAB+) ionization detection simultaneously. Samples were diluted 1−50 times with water or MeCN and injected directly into the source. Crystallographic analysis was conducted at the organometallic laboratory at Seoul National University.

***tert*-Butyl 2-(2-Nitroimidazolyl)ethylcarbamate.** K_2CO_3 (1.83 g, 13.26 mmol) was added to a stirring solution of **1** (1 g, 8.84 mmol) in DMF (3 mL). *tert*-Butyl 2-bromoethylcarbamate (1.98 g, 8.84 mmol) was then added dropwise, and the reaction mixture was stirred at room temperature overnight. The reaction mixture was than filtered, the solid obtained was washed with MeOH, and residual solvent was evaporated. The solid obtained was dissolved in water, extracted with EtOAc, and the organic layer was evaporated in vacuo to obtain the solid. Finally the crude compound was recrystallized from EtOAc to afford pure compound as a dark yellow solid (1.9 g, 84%), and purity was confirmed by TLC. ^{1}H NMR (CD_3OD): δ 7.35 (s, 1H), 7.10 (s, 1H), 4.51−4.54 (t, J = 9 Hz, 2H), 3.47−3.50 (t, J = 9 Hz, 2H), 1.28-1.39 (s, 9H). ^{13}C NMR (CD_3OD): δ 158.4, 131.9, 129, 128.3, 80.4, 51.2, 40.8, 28.7. MS (ESI$^+$), (M + Na)$^+$: 279.1 observed, 279.11 calculated for $C_{10}H_{16}N_4NaO_4$.

2-(2-Nitroimidazolyl)ethylamine (2). A sample of 1.25 M HCl in MeOH (3 mL) was added to a solution of *tert*-butyl 2-(2-nitroimidazolyl)ethylcarbamate (1.9 g) in MeOH (2 mL) at room temperature under continuous stirring. After 5 h the resulting product **2** was filtered and washed with MeOH and evaporated in vacuo. The solid obtained was recrystallized from MeOH to afford pure compound **2** as a pale yellow solid (1.2 g, 84%). TLC was used to confirm the purity, where the product appeared as a single spot in TLC. ^{1}H NMR (CD_3OD): δ 7.56 (s, 1H), 7.21 (s, 1H), 4.75−4.79 (t, J = 12 Hz, 2H), 3.47−3.51 (t, J = 12 Hz, 2H). ^{13}C NMR (CD_3OD): δ 145.2, 128.8, 128.5, 47.2, 39.7. MS (ESI$^+$), (M + H)$^+$: 157.1 observed, 157.07 calculated for $C_5H_9N_4O_2$.

NOTA-2-NI-*N*-ethylamine (3). A solution of **2** (0.021 g, 0.1 mmol) in DMF (3 mL) and DCC (0.034 g, 0.16 mmol) solution in pyridine (0.5 mL) were sequentially added to NOTA (0.050 g, 0.16 mmol) solution in water (3 mL) with stirring. The reaction mixture was then stirred at room temperature overnight and filtered. The aqueous solution was evaporated in vacuo and purified by RP-HPLC (100% of A for 5 min and 0−60% of C for 30 min) to obtain pure compound **3** as a white solid (25 mg, 52%). After purification, the product obtained was injected into an analytical HPLC column with the same conditions used for the purification and found to be single peak, and also purity was confirmed by HRMS. ^{1}H NMR (300 MHz, D_2O): δ 7.31 (s, 1H), 7.02 (s, 1H), 4.46 (br, 2H), 3.78 (br, 4H), 3.56 (br, 4H), 3.25 (br, 4H), 3.14 (br, 4H), 2.96 (br, 4H). ^{13}C NMR (75 MHz, D_2O): δ 172.2, 172.0, 145.3, 129.3, 128.1, 58.3, 57.0, 51.3, 50.7, 50.4, 50.0, 39.2. MS (ESI$^+$), (M + H)$^+$: 442.1 observed, 442.21 calculated. HRMS: 442.2055 observed, 442.2050 calculated for $C_{17}H_{28}N_7O_7$.

SCN-NOTA-2-NI-*N*-ethylamine (4). A mixture of SCN-NOTA (0.05 g, 0.11 mmol) and **2** (0.026 g, 0.13 mmol) in $CHCl_3$ (1 mL) containing TEA (0.034 g, 0.33 mmol; used as a base) was stirred overnight at room temperature. The resulting product was purified by RP-HPLC (30−60% of C with A for 30 min) to afford **4** as light yellow solid (49 mg, 73%). The product purity was confirmed by analytical HPLC (with the same conditions) as well as by HRMS. ^{1}H NMR (D_2O): δ 7.13−7.06 (d, 3H), 6.92−6.87 (d, 3H), 4.39 (br, 3H), 3.80−3−69 (br, 6H), 3.41−3.34 (q, 1H), 3.21−3.13 (br, 7H), 2.97−2.90 (br, 3H), 2.61−2.45 (br, 1H), 1.03−0.98 (t, 1H), 0.93−0.88 (t, 1H). ^{13}C NMR (D_2O): δ 181.1, 176.4, 172.3, 171.0, 145.2, 130.9, 129.4, 128.4, 128.3, 126.8, 58.0, 56.4, 54.3, 52.5, 50.1, 47.2, 43.9, 43.2, 43.0, 34.0, 30.7. MS (ESI$^+$), (M + H)$^+$: 607.1 observed, 607.23 calculated. HRMS: 607.2307 observed, 607.2302 calculated for $C_{25}H_{35}N_8O_8S$.

Ga-NOTA-NI Complex (Ga-3). $Ga(NO_3)_3 \cdot xH_2O$ and **3** were dissolved in water at a stoichiometric ratio of 1:1, and the pH was adjusted to 5 by adding 0.5 M Na_2CO_3 solution using microfine pH test paper. This mixture was then heated in a boiling water bath for 30 min. In addition, the same procedure was repeated at pH 3. MS/ESI$^+$ was used to confirm reaction completion and was purified by RP-HPLC (15−30% of D with B for 30 min) and lyophilized to afford Ga-**3** as a white solid. The purity confirmation was done by analytical HPLC. ^{1}H NMR (D_2O): δ 7.35 (s, 1H), 7.11 (s, 1H), 4.57 (br, 2H), 4.10 (br, 2H), 3.90 (br, 2H), 3.60−3.74 (q, 4H), 3.34 (br, 6H), 3.03 (br, 4H), 2.80 (br, 2H). MS (ESI$^+$), (M + H)$^+$: 508.1 observed, 508.11 calculated $C_{17}H_{25}GaN_7O_7$.

X-ray Diffraction Analysis. Data Reduction. Single crystal diffraction data were obtained using an Enraf-Nonius CCD single-crystal X-ray diffractometer at room temperature using graphite-monochromated Mo Kα radiation (λ = 0.710 73 Å). Preliminary orientation matrices and unit cell parameters were obtained from the peaks of the first 10 frames and then refined using whole data sets. Frames were integrated and corrected for Lorentz and polarization effects using DENZO-SMN.[50]

Structure Solution and Refinement. The structures of the crystals were solved by direct methods using SHELXS-97 and refined by full-matrix least-squares with SHELXL-97.[51] Drawings were prepared using ORTEP[52] software. All non-hydrogen atoms were refined anisotropically. All hydrogen atoms are treated as idealized contributions.

Radionuclide Labeling. NaOAc buffer (1 M, pH 5, 0.1 mL) was added to **3** (22 μg) in 0.1 mL of $^{68}GaCl_3$ (39.6−245.3 MBq), which was eluted from a ^{68}Ge/^{68}Ga-generator using 0.1 M HCl to adjust the pH to ~3, and then the mixture was heated at 100 °C for 10 min. The reaction mixture was analyzed by ITLC-SG (German Science, Ann Arbor, MI) using 0.1 M Na_2CO_3 solution as eluant to check labeling efficiency (Supporting Information Figure 1). ^{68}Ga-**4** (50 nmol) was labeled using $^{68}GaCl_3$ (150.2−355.2 MBq) and the same procedure.

Stability Study. The above prepared ^{68}Ga-**3** and ^{68}Ga-**4** were stored at room temperature for 0, 30, 60, 120, and 240 min and then analyzed by ITLC-SG: 0.1 M Na_2CO_3 ($^{68}Ga^{3+}$ remained at the origin, and labeled products moved with the solvent front) and 0.1 M HCl ($^{68}Ga^{3+}$ moved with the solvent front,

and labeled products remained at the origin) were used as eluants.

Partition Coefficients. Na_2PO_4 buffer (0.1 M, pH 7.4, 3 g) was added to octanol (3 g), and then ^{68}Ga-**3** (1.1 MBq/10 μL) or ^{68}Ga-**4** (1.2 MBq/10 μL) was added, mixed vigorously, and centrifuged (3000 rpm for 5 min). Radioactivities of octanol fraction (0.5 g) and 0.1 M Na_2PO_4 buffer fraction (0.5 g) were measured using a γ counter, and log *P* values were calculated.

Serum Protein Binding. Human serum protein binding fractions were determined using a previously reported method with minor modifications.[48] PD-10 columns were preconditioned by loading 1.0 mL of 1% bovine serum albumin in 0.1 M DTPA and successive washing with 100 mL of phosphate buffered saline (PBS). ^{68}Ga-**3** (1.3 MBq/10 μL) or ^{68}Ga-**4** (1.1 MBq/10 μL) was mixed with human serum (1 mL) and incubated for 10 or 60 min at 37 °C. And then each mixture was loaded onto a preconditioned PD-10 column and eluted with PBS; 30 fractions (fraction size 0.5 mL) were collected per sample in 5 mL test tubes. Radioactivity of each fraction was measured using a γ counter and expressed as cpm (count per minute). To check for the presence of protein in each fraction, aliquots (2 μL) from each test tube were spotted on a filter paper and stained with Coomassie blue. Protein bound fractions appeared at the void volume and free fractions at the bed volume.

In Vitro Cell Uptake Study. Cell uptake studies were carried out using the CHO and CT-26 cell lines. Both cell lines were maintained in DMEM culture medium enriched with 10% fetal bovine serum (both from Welgene Inc., Korea) and containing a 1% antibiotics mixture (penicillin, streptomycin, and amphotericin B: (10 000 IU/10 mg)/25 μg/mL, Mediatech Inc.) in 5% CO_2 in an incubator at 37 °C. The cells were subcultured overnight in 24-well plates (2×10^5 cells/well). And then preincubation was performed under normoxic (5% CO_2 in air) or hypoxic (5% CO_2 in 95% N_2) conditions for 4 h. ^{68}Ga-**3** (0.37 MBq/100 μL) or ^{68}Ga-**4** (0.44 MBq/100 μL) was added to the wells and incubated for 5 or 60 min. Wells were then washed with DMEM (Dulbecco's modified Eagle medium), and the cells were dissolved in 0.5% of SDS (sodium dodecyl sulfate) in PBS (phosphate buffered saline) (0.5 mL). The tracer uptakes were measured using a γ-counter (Packard, Canberra Co.), and total protein concentrations in samples were determined using the bicinchoninic acid method (Pierce).

Biodistribution in Mice Bearing Colon Cancer Xenografts. All animal experiments were performed with the approval of the Institutional Animal Care and Use Committee of the Clinical Research Institute at Seoul National University Hospital (an Association for Assessment and Accrediation of Laboratory Animal Care accrediated facility). In addition, National Research Council guidelines for the care and use of laboratory animals (revised in 1996) were observed throughout. The mouse colon cancer cell line CT-26 was grown in RPMI 1640 medium containing 10% fetal bovine serum and harvested after treatment with trypsin. Cells were washed with 10 mL of PBS by centrifugation (3000 rpm). Each Balb/c mouse was injected subcutaneously with (2×10^5)/0.1 mL CT-26 cells in the right shoulder. After 13 days, ^{68}Ga-labeled agents (37 KBq/0.1 mL) were injected intravenously into each xenografted mouse. Mice were sacrificed at different time intervals (10, 30, 60, and 120 min) after injection. Tumor, blood, muscle, and other organs were separated immediately and weighed, and counts were obtained with a γ-scintillation counter. Results were expressed as the percentage injected dose per gram of tissue (% ID/g).

PET of Tumor Bearing Mice. CT-26 cells (2×10^5 cells) in normal saline (0.1 mL) were subcutaneously injected into the mice right shoulders and grown for 14 days to produce tumors of diameter of ~16 mm. ^{68}Ga-**3** (13.3 MBq/0.1 mL) or ^{68}Ga-**4** (12.6 MBq/0.1 mL) was intravenously injected through a tail vein. Mice were anesthetized with 2% isoflurane at 30 and 60 min, and PET images were then obtained. PET studies were performed using a dedicated small-animal PET/CT scanner (GE Healthcare, Princeton, NJ). Emission data were acquired for 20 min. The acquired three-dimensional emission raw data were reconstructed to temporally framed sonograms by Fourier rebinning using ordered subsets expectation maximization (OSEM) reconstruction algorithm without attenuation correction. For the PET images, data were analyzed in 20 frames (10 times with 1 min frames).

Data Analysis. AsiPRO VM 5.0 software (Concorde Microsystems, Knoxville, TN) was used to perform image and region of interest (ROI) analyses with the PET data sets. For the ROI (value/pixel) analyses, 1.5 mm radius of sphere per tumor and muscle were collected, and ROI and standard deviation were determined. Once ROI determination was done, SUV was calculated using the formula

$$\mathrm{SUV} = \mathrm{CCF}/(\text{injected dose/weight of mouse})$$

where CCF (decay corrected activity concentration) was calculated by the formula

$$\mathrm{CCF}\ (\mathrm{MBq/mL}) = \text{radioactivity (mCi/mL)} \times \text{branching ratio} \times \text{RIO (value/pixel)}$$

where the branching ratio for ^{68}Ga is 0.891.

Acknowledgment. This work was supported by NRF of Korea (Grants R0A-2008-000-20116-0 and 2009-0082087), funded by Ministry of Education, Science and Technology.

Note Added after ASAP Publication. This paper was published on the Web on August 6, 2010 with several minor textual errors. The revised version was published on August 11, 2010.

Supporting Information Available: Labeling experiments and stability data, crystallographic information, and analytical and spectral characterization data. This material is available free of charge via the Internet at http://pubs.acs.org.

References

(1) Lucignani, G. PET imaging with hypoxia tracers: a must in radiation therapy. *Eur. J. Nucl. Med. Mol. Imaging* **2008**, *35*, 838–842.
(2) Martin, G. V.; Caldwell, J. H.; Graham, M. M.; Grierson, J. R.; Kroll, K.; Cowan, M. J.; Lewellen, T. K.; Rasey, J. S.; Casciari, J. J.; Krohn, K. A. Noninvasive detection of hypoxic myocardium using fluorine-18-fluoromisonidazole and positron emission tomography. *J. Nucl. Med.* **1992**, *33*, 2202–2208.
(3) Shi, C. Q.; Sinusas, A. J.; Dione, D. P.; Singer, M. J.; Young, L. H.; Heller, E. N.; Rinker, B. D.; Wackers, F. J.; Zaret, B. L. Technetium-99m-nitroimidazole (BMS181321): a positive imaging agent for detecting myocardial ischemia. *J. Nucl. Med.* **1995**, *36*, 1078–1086.
(4) Barthel, H.; Wilson, H.; Collingridge, D. R.; Brown, G.; Osman, S.; Luthra, S. K.; Brady, F.; Workman, P.; Price, P. M.; Aboagye, E. O. In vivo evaluation of [^{18}F]fluoroetanidazole as a new marker for imaging tumour hypoxia with positron emission tomography. *Br. J. Cancer* **2004**, *90*, 2232–2242.
(5) Nunn, A.; Linder, K.; Strauss, H. Nitroimidazoles and imaging hypoxia. *Eur. J. Nucl. Med. Mol. Imaging* **1995**, *22*, 265–280.
(6) Piert, M.; Machulla, H. J.; Picchio, M.; Reischl, G.; Ziegler, S.; Kumar, P.; Wester, H. J.; Beck, R.; McEwan, A. J. B.; Wiebe, L. I.; Schwaiger, M. Hypoxia-specific tumor imaging with F-18-fluoroazomycin arabinoside. *J. Nucl. Med.* **2005**, *46*, 106–113.
(7) Reischl, G.; Dorow, D. S.; Cullinane, C.; Katsifis, A.; Roselt, P.; Binns, D.; Hicks, R. J. Imaging of tumor hypoxia with [I-124]IAZA in comparison with [F-18]FMISO and [F-18]FAZA—first small animal PET results. *J. Pharm. Pharm. Sci.* **2007**, *10*, 203–211.
(8) Reischl, G.; Ehrlichmann, W.; Bieg, C.; Solbach, C.; Kumar, P.; Wiebe, L. I.; Machulla, H. J. Preparation of the hypoxia imaging PET tracer [^{18}F]FAZA: reaction parameters and automation. *Appl. Radiat. Isot.* **2005**, *62*, 897–901.
(9) Tewson, T. Synthesis of [^{18}F]fluoroetanidazole: a potential new tracer for imaging hypoxia. *Nucl. Med. Biol.* **1997**, *24*, 755–760.
(10) Mallia, M.; Subramanian, S.; Mathur, A.; Sarma, H.; Venkatesh, M.; Banerjee, S. On the isolation and evaluation of a novel

unsubstituted 5-nitroimidazole derivative as an agent to target tumor hypoxia. *Bioorg. Med. Chem. Lett.* **2008**, *18*, 5233–5237.
(11) Melo, T.; Duncan, J.; Ballinger, J. R.; Rauth, A. M. BRU59-21, a second-generation Tc-99m-labeled 2-nitroimidazole for imaging hypoxia in tumors. *J. Nucl. Med.* **2000**, *41*, 169–176.
(12) Oswald, J.; Treite, F.; Haase, C.; Kampfrath, T.; Mäding, P.; Schwenzer, B.; Bergmann, R.; Pietzsch, J. Experimental hypoxia is a potent stimulus for radiotracer uptake in vitro: comparison of different tumor cells and primary endothelial cells. *Cancer Lett.* **2007**, *254*, 102–110.
(13) Rajendran, J. G.; Hendrickson, K. R. G.; Spence, A. M.; Muzi, M.; Krohn, K. A.; Mankoff, D. A. Hypoxia imaging-directed radiation treatment planning. *Eur. J. Nucl. Med. Mol. Imaging* **2006**, *33*, S44–S53.
(14) Riche, F.; du Moulinet d'Hardemare, A.; Sèpe, S.; Riou, L.; Fagret, D.; Vidal, M. Nitroimidazoles and hypoxia imaging: synthesis of three technetium-99m complexes bearing a nitroimidazole group: biological results. *Bioorg. Med. Chem. Lett.* **2001**, *11*, 71–74.
(15) Zhang, X. G.; Melo, T.; Rauth, A. M.; Ballinger, J. R. Cellular accumulation and retention of the technetium-99m-labelled hypoxia markers BRU59-21 and butylene amine oxime. *Nucl. Med. Biol.* **2001**, *28*, 949–957.
(16) Ziemer, L.; Evans, S.; Kachur, A. Noninvasive imaging of tumor hypoxia using the 2-nitroimidazole [^{18}F]EF5 in rats. *Eur. J. Nucl. Med.* **2003**, *30*, 259–266.
(17) Takasawa, M.; Moustafa, R. R.; Baron, J. C. Applications of nitroimidazole in vivo hypoxia imaging in ischemic stroke. *Stroke* **2008**, *39*, 1629–1637.
(18) Sorger, D.; Patt, M.; Kumar, P.; Wiebe, L. I.; Barthel, H.; Seese, A.; Dannenberg, C.; Tannapfel, A.; Kluge, R.; Sabri, O. [^{18}F]Fluoroazomycinarabinofuranoside (^{18}FAZA) and [^{18}F]fluoromisonidazole (^{18}FMISO): a comparative study of their selective uptake in hypoxic cells and PET imaging in experimental rat tumors. *Nucl. Med. Biol.* **2003**, *30*, 317–326.
(19) Rauth, A. M.; Melo, T.; Misra, V. Bioreductive therapies: an overview of drugs and their mechanisms of action. *Int. J. Radiat. Oncol., Biol., Phys.* **1998**, *42*, 755–762.
(20) Lee, S. T.; Scott, A. M. Hypoxia positron emission tomography imaging with ^{18}F-fluoromisonidazole. *Semin. Nucl. Med.* **2007**, *37*, 451–461.
(21) Martin, G. V.; Caldwell, J. H.; Rasey, J. S.; Grunbaum, Z.; Cerqueira, M.; Krohn, K. A. Enhanced binding of the hypoxic cell marker [^{3}H]fluoromisonidazole in ischemic myocardium. *J. Nucl. Med.* **1989**, *30*, 194–201.
(22) Rajendran, J. G.; Schwartz, D. L.; O'Sullivan, J.; Peterson, L. M.; Ng, P.; Scharnhorst, J.; Grierson, J. R.; Krohn, K. A. Tumor hypoxia imaging with [F-18]fluoromisonidazole positron emission tomography in head and neck cancer. *Clin. Cancer Res.* **2006**, *12*, 5435–5441.
(23) Shelton, M. E.; Dence, C. S.; Hwang, D. R.; Welch, M. J.; Bergmann, S. R. Myocardial kinetics of fluorine-18 misonidazole: a marker of hypoxic myocardium. *J. Nucl. Med.* **1989**, *30*, 351–358.
(24) Yang, D. J.; Wallace, S.; Cherif, A.; Li, C.; Gretzer, M. B.; Kim, E. E.; Podoloff, D. A. Development of F-18-labeled fluoroerythronitroimidazole as a PET agent for imaging tumor hypoxia. *Radiology* **1995**, *194*, 795–800.
(25) Gronroos, T.; Bentzen, L.; Marjamaki, P.; Murata, R.; Horsman, M. R.; Keiding, S.; Eskola, O.; Haaparanta, M.; Minn, H.; Solin, O. Comparison of the biodistribution of two hypoxia markers [^{18}F]FETNIM and [^{18}F]FMISO in an experimental mammary carcinoma. *Eur. J. Nucl. Med. Mol. Imaging* **2004**, *31*, 513–520.
(26) Grosu, A. L.; Souvatzoglou, M.; Roper, B.; Dobritz, M.; Wiedenmann, N.; Jacob, V.; Wester, H. J.; Reischl, G.; Machulla, H. J.; Schwaiger, M.; Molls, M.; Piert, M. Hypoxia imaging with FAZA-PET and theoretical considerations with regard to dose painting for individualization of radiotherapy in patients with head and neck cancer. *Int. J. Radiat. Oncol., Biol., Phys.* **2007**, *69*, 541–551.
(27) Postema, E. J.; McEwan, A. J.; Riauka, T. A.; Kumar, P.; Richmond, D. A.; Abrams, D. N.; Wiebe, L. I. Initial results of hypoxia imaging using 1-alpha-D: -(5-deoxy-5-[^{18}F]-fluoroarabinofuranosyl)-2-nitroimidazole (^{18}F-FAZA). *Eur. J. Nucl. Med. Mol. Imaging* **2009**, *36*, 1565–1573.
(28) Souvatzoglou, M.; Grosu, A. L.; Roper, B.; Krause, B. J.; Beck, R.; Reischl, G.; Picchio, M.; Machulla, H. J.; Wester, H. J.; Piert, M. Tumour hypoxia imaging with [^{18}F]FAZA PET in head and neck cancer patients: a pilot study. *Eur. J. Nucl. Med. Mol. Imaging* **2007**, *34*, 1566–1575.
(29) Komar, G.; Seppanen, M.; Eskola, O.; Lindholm, P.; Gronroos, T. J.; Forsback, S.; Sipila, H.; Evans, S. M.; Solin, O.; Minn, H. ^{18}F-EF5: a new PET tracer for imaging hypoxia in head and neck cancer. *J. Nucl. Med.* **2008**, *49*, 1944–1951.
(30) Yapp, D. T.; Woo, J.; Kartono, A.; Sy, J.; Oliver, T.; Skov, K. A.; Koch, C. J.; Adomat, H.; Dragowska, W. H.; Fazli, L.; Ruth, T.; Adam, M. J.; Green, D.; Gleave, M. Non-invasive evaluation of tumour hypoxia in the Shionogi tumour model for prostate cancer with ^{18}F-EF5 and positron emission tomography. *BJU Int.* **2007**, *99*, 1154–1160.
(31) Dolbier, W. R., Jr.; Li, A. R.; Koch, C. J.; Shiue, C. Y.; Kachur, A. V. [^{18}F]-EF5, a marker for PET detection of hypoxia: synthesis of precursor and a new fluorination procedure. *Appl. Radiat. Isot.* **2001**, *54*, 73–80.
(32) Bussink, J.; van der Kogel, A. J.; Kaanders, J. H. Patterns and levels of hypoxia in head and neck squamous cell carcinomas and their relationship to patient outcome: in regard to Evans et al. (Int. J. Radiat. Oncol. Biol. Phys. 2007; 69: 1024−1031). *Int. J. Radiat. Oncol. Biol. Phys.* **2008**, *70*, 1616.
(33) Lewis, J.; Laforest, R.; Dehdashti, F.; Grigsby, P.; Welch, M.; Siegel, B. An imaging comparison of ^{64}Cu-ATSM and ^{60}Cu-ATSM in cancer of the uterine cervix. *J. Nucl. Med.* **2008**, *49*, 1177.
(34) Lewis, J. S.; McCarthy, D. W.; McCarthy, T. J.; Fujibayashi, Y.; Welch, M. J. Evaluation of Cu-64-ATSM in vitro and in vivo in a hypoxic tumor model. *J. Nucl. Med.* **1999**, *40*, 177–183.
(35) V vere, A.; Lewis, J. Cu-ATSM: a radiopharmaceutical for the PET imaging of hypoxia. *Dalton Trans.* **2007**, 4893–4902.
(36) Breeman, W. A. P.; Verbruggen, A. M. The Ge-68/Ga-68 generator has high potential, but when can we use Ga-68-labelled tracers in clinical routine? *Eur. J. Nucl. Med. Mol. Imaging* **2007**, *34*, 978–981.
(37) Maecke, H. R.; Hofmann, M.; Haberkorn, U. Ga-68-labeled peptides in tumor imaging. *J. Nucl. Med.* **2005**, *46*, 172s–178s.
(38) Riss, P. J.; Kroll, C.; Nagel, V.; Rosch, F. NODAPA-OH and NODAPA-(NCS)(n): synthesis, Ga-68-radiolabelling and in vitro characterisation of novel versatile bifunctional chelators for molecular imaging. *Bioorg. Med. Chem. Lett.* **2008**, *18*, 5364–5367.
(39) Velikyan, I.; Maecke, H.; Langstrom, B. Convenient preparation of ^{68}Ga-based PET-radiopharmaceuticals at room temperature. *Bioconjugate Chem.* **2008**, *19*, 569–573.
(40) Yang, B. Y.; Jeong, J. M.; Kim, Y. J.; Choi, J. Y.; Lee, Y. S.; Lee, D. S.; Chung, J. K.; Lee, M. C. Formulation of ^{68}Ga BAPEN kit for myocardial positron emission tomography imaging and biodistribution study. *Nucl. Med. Biol.* **2010**, *37*, 149–155.
(41) Craig, A. S.; Parker, D.; Adams, H.; Bailey, N. A. Stability, Ga-71 NMR, and crystal-structure of a neutral gallium(III) complex of 1,4,7-triazacyclononanetriacetate, a potential radiopharmaceutical. *J. Chem. Soc., Chem. Commun.* **1989**, 1793–1794.
(42) Prata, M.; Santos, A.; Geraldes, C.; de Lima, J. Structural and in vivo studies of metal chelates of Ga (III) relevant to biomedical imaging. *J. Inorg. Biochem.* **2000**, *79*, 359–363.
(43) Wu, C.; Jagoda, E.; Brechbiel, M.; Webber, K.; Pastan, I.; Gansow, O.; Eckelman, W. Biodistribution and catabolism of Ga-67-labeled anti-Tac dsFv fragment. *Bioconjugate Chem.* **1997**, *8*, 365–369.
(44) Jeong, J. M.; Hong, M. K.; Chang, Y. S.; Lee, Y. S.; Kim, Y. J.; Cheon, G. J.; Lee, D. S.; Chung, J. K.; Lee, M. C. Preparation of a promising angiogenesis PET imaging agent: Ga-68-labeled c(RGDyK)-isothiocyanatobenzyl-1,4,7-triazacyclononane-1,4,7-triacetic acid and feasibility studies in mice. *J. Nucl. Med.* **2008**, *49*, 830–836.
(45) Norman, T. J.; Smith, F. C.; Parker, D.; Harrison, A.; Royle, L.; Walker, C. A. Synthesis and biodistribution of In-111, Ga-67 and Gd-153-radiolabeled conjugates of nitroimidazoles with bifunctional complexing agents—imaging agents for hypoxic tissue. *Supramol. Chem.* **1995**, *4*, 305–308.
(46) Andre, J. P.; Maecke, H. R.; Zehnder, M.; Macko, L.; Akyel, K. G. 1,4,7-Triazacyclononane-1-succinic acid-4,7-diacetic acid (NODASA): a new bifunctional chelator for radio gallium-labelling of biomolecules. *Chem. Commun.* **1998**, 1301–1302.
(47) Jyo, A.; Kohno, T.; Terazono, Y.; Kawano, S. Crystal-structure of gallium(III) complex of 1,4,7-triazacyclononane-*N*,*N*-$'$,*N*-$''$-triacetate. *Anal. Sci.* **1990**, *6*, 323–324.
(48) Jeong, J. M.; Kim, Y. J.; Lee, Y. S.; Lee, D. S.; Chung, J. K.; Lee, M. C. Radiolabeling of NOTA and DOTA with positron emitting ^{68}Ga and investigation of in vitro properties. *Nucl. Med. Mol. Imaging* **2009**, *43*, 330–336.
(49) Liu, R.; Chou, T.; Chang, C.; Wu, C.; Chang, C.; Chang, T.; Wang, S.; Lin, W.; Wang, H. Biodistribution, pharmacokinetics and PET imaging of [^{18}F]FMISO, [^{18}F]FDG and [^{18}F]FAc in a sarcoma- and inflammation-bearing mouse model. *Nucl. Med. Biol.* **2009**, *36*, 305–312.
(50) Otwinowski, Z.; Minor, W. Processing of X-ray diffraction data collected in oscillation mode. *Methods Enzymol.* **1997**, 307–325.
(51) Sheldrick, G. *SHELXs97 and SHELXL97*; University of Göttingen: Göttingen, Germany, 1997.
(52) Johnson, C. ORTEPII. Report ORNL-5138; Oak Ridge National Laboratory: Oak Ridge, TN, 1976; p 1718.